*organoids*

MDPI

*Article*

# Paraffin Embedding and Histological Analyses of Sw71-Spheroids as Human Blastocyst-like Surrogates

**Marina Alexandrova, Mariela Ivanova, Martina Metodieva, Antonia Terzieva and Tanya Dimova ***

Institute of Biology and Immunology of Reproduction "Acad. Kiril Bratanov", Bulgarian Academy of Sciences, 73 Tzarigradsko Shosse, 1113 Sofia, Bulgaria; marina.m.alexandrova@gmail.com (M.A.); mariela.ivanova021@gmail.com (M.I.); martina.metodieva@hotmail.com (M.M.); anterzieva@abv.bg (A.T.)
* Correspondence: tanyadimova@yahoo.com

**Abstract**

Implantation studies are extremely important to solve reproductive problems since about 60% of abortions occur around this period. The 3D in vitro models emerge as closest to the in vivo structures and processes. Here, we constructed trophoblast Sw71-spheroids as implanting human blastocyst–like surrogates (BLS). The model is well-characterized, standardized, validated tool to study extravillous trophoblast (EVT) invasion/migration during implantation. A limitation is that it is a short-living 3D-culture that must be generated de novo. This study aimed to create and embed Sw71-spheroids in paraffin for permanent histological preparations. The main challenges were the micro-size and the preservation of the intact structure. The standardly generated compact and stable Sw71-spheroids were intact, with blastocyst-like morphology. Histological analysis showed preserved cell morphology, shape, and intact periphery of the embedded Sw71-spheroids. These were usable for immunohistochemistry(IHC) and expressed common EVT markers: EpCAM, HLA-C and and HLA-G. Our protocol for spheroid paraffin embedding is suitable for simultaneous histological analyses of several Sw71-spheroids. It might be further optimized to embed migrating/invading Sw71-BLS as snapshots of trophoblast implantation steps in permanent histological preparations for in depth IHC studies.

**Keywords:** Sw71-spheroids; paraffin-embedding; HLA molecules

check for updates

Academic Editor: Süleyman Ergün

Received: 15 April 2025
Revised: 1 July 2025
Accepted: 6 August 2025
Published: 11 August 2025

**Citation:** Alexandrova, M.; Ivanova, M.; Metodieva, M.; Terzieva, A.; Dimova, T. Paraffin Embedding and Histological Analyses of Sw71-Spheroids as Human Blastocyst-like Surrogates. *Organoids* **2025**, *4*, 19. https://doi.org/10.3390/organoids4030019

**Copyright:** © 2025 by the authors. Licensee MDPI, Basel, Switzerland. This article is an open access article distributed under the terms and conditions of the Creative Commons Attribution (CC BY) license (https://creativecommons.org/licenses/by/4.0/).

## 1. Introduction

Human implantation is a process difficult to observe directly in both natural and assisted reproduction. It was summarized that about 60% of abortions occur namely around/in the implantation period [1–4]. Therefore, implantation studies are extremely important to solve reproductive problems. All available in vivo, ex vivo and in vitro human implantation models have their pros and cons. Lately the biotechnology in the field of reproductive sciences has made a tremendous progress. The three dimensional (3D) in vitro models such as spheroids, blastoids and organoids show up as the best alternative to better understand complex biology in a physiologically relevant context in in vivo structures and processes [5–7]. The creation of surrogates of the human blastocyst has attracted great interest [6]. These are designed to resemble the earliest stages of human embryo development, even before the pregnancy is registered. Moreover, these models could help to avoid the ethical constraints for the use of human embryos and their derivatives for science [8]. They have great potential for a variety of applications—from expanding our knowledge of human development to possibly improving assisted reproduction methods [6].

In the previous research we and others described the generation of Sw71-spheroids as implanting human blastocyst–like surrogates (BLS) [9–11] from the normal, immortalized, Sw71 (#CVCL_D855) trophoblast cell line isolated from 1st trimester human placenta [12]. Sw71-spheroids are well-characterized, standardized, reproducible, validated, and reliable tool to study/model extravillous trophoblast (EVT) function during implantation [6,9–11,13]. It is known to resemble the size and shape of the expanded, implanting human blastocyst after compactization and cavitation [6,9]. The Sw71-spheroid EVT-like cells function alike the differentiating EVT of the blastocyst during implantation. They migrate and invade the extracellular matrix, and between endometrial stromal cells [6,9–11,13]. Moreover, the Sw71-BLS model is validated against the corresponding 3D model from isolated primary EVT for a specific CK7+/Vim+/HLA-C+/HLA-G+ profile. It allows these EVT-like trophoblasts to be able for constant epithelial-mesenchymal and reverse transitions, just like the primary EVT do. These transitions conduct the invasion of the decidua during the implantation and remodeling of uterine spiral arteries [13,14]. A limitation is that the model is a short-living 3D culture and must be generated de novo for the experiments [9]. Formalin-fixed paraffin-embedded (FFPE) samples are easy to handle and store for many years at room temperature (RT). The main challenges of using paraffin-embedded spheroid cultures are the micro-size of the object and the optimal fixation, complete dehydration and paraffin infiltration to obtain the intact structures with preserved proteins for subsequent analyses.

This study aimed to create de novo trophoblast Sw71-spheroids and embed them in paraffin for permanent histological preparations for further and in-depth studies on the trophoblast of the implanting blastocyst.

## 2. Materials and Methods

### *2.1. Differentiation of Sw71-Spheroids as Blastocyst-like Surrogates*

We used normal, immortalized, 1st-trimester human placenta Sw71 (#CVCL_D855) trophoblast cell line [12]. The Sw71-spheroids were differentiated following standard protocol [9,11]. In brief, Sw71-BLS were differentiated from 4000 Sw71 cells/well in ultra-low attachment plate (ULA, Costar, Amsterdam, The Netherlands) after centrifugation (5 min/370× *g*) and subsequent incubation in DMEM-F12 complete medium for 48 h, at 37 °C, 5%$CO_2$. The differentiation media (#D8062, Sigma-Aldrich, Taufkirchen, Germany) was supplemented with 10% heat-inactivated fetal calf serum (FCS, Ref.: F7524, Sigma-Aldrich, Taufkirchen, Germany), 10 mmol/L HEPES (Ref.: H0887, Sigma-Aldrich, Taufkirchen, Germany), 0.1 mmol/L MEM non-essential amino acids (Ref.: M7145, Sigma-Aldrich, Taufkirchen, Germany), 1 mmol/L sodium pyruvate (Ref.: 11360-039, Gibco, Waltham, MA USA), and 100 U/mL penicillin/streptomycin (Ref.: 4458, Sigma-Aldrich). The dynamic process of Sw71-spheroid differentiation was monitored with time-lapse live cells imaging system Omni (Axion Biosystems, Inc., Atlanta, GA, USA) and captured every 24 h with ECHO Revolve microscope (RVL100-M, Echo, San Diego, CA, USA). Their morphology and size were assessed by the mean diameter and the spheroid surface on day 0, to day 2, as previously described [9]. In brief the mean diameter of a single Sw71-BLS is calculated as the average of the two largest diameters since the model is not a perfect sphere. The surface is directly determined with the ECHO software (RVL100-M, Echo, San Diego, CA, USA). Only stable, spherical structures with intact periphery and size around 350 µm were selected. Some of the selected Sw71 spheroids were tested for migration and invasion to be proved as functional and viable. We used established protocols [11]. We did not test the spheroids for apoptosis and necrosis prior to sectioning.

### 2.2. Paraffin Embedding of Sw71-BLS

The structures were proceeded to obtain FFPE Sw71 spheroids paraffin sections. The workflow chart with the steps of the protocol is shown in Figure 1. In addition, we directly embedded Sw71 spheroids in paraffin without pre-embedding (without step 3, Figure 1. Three independent preparations were performed for each condition.

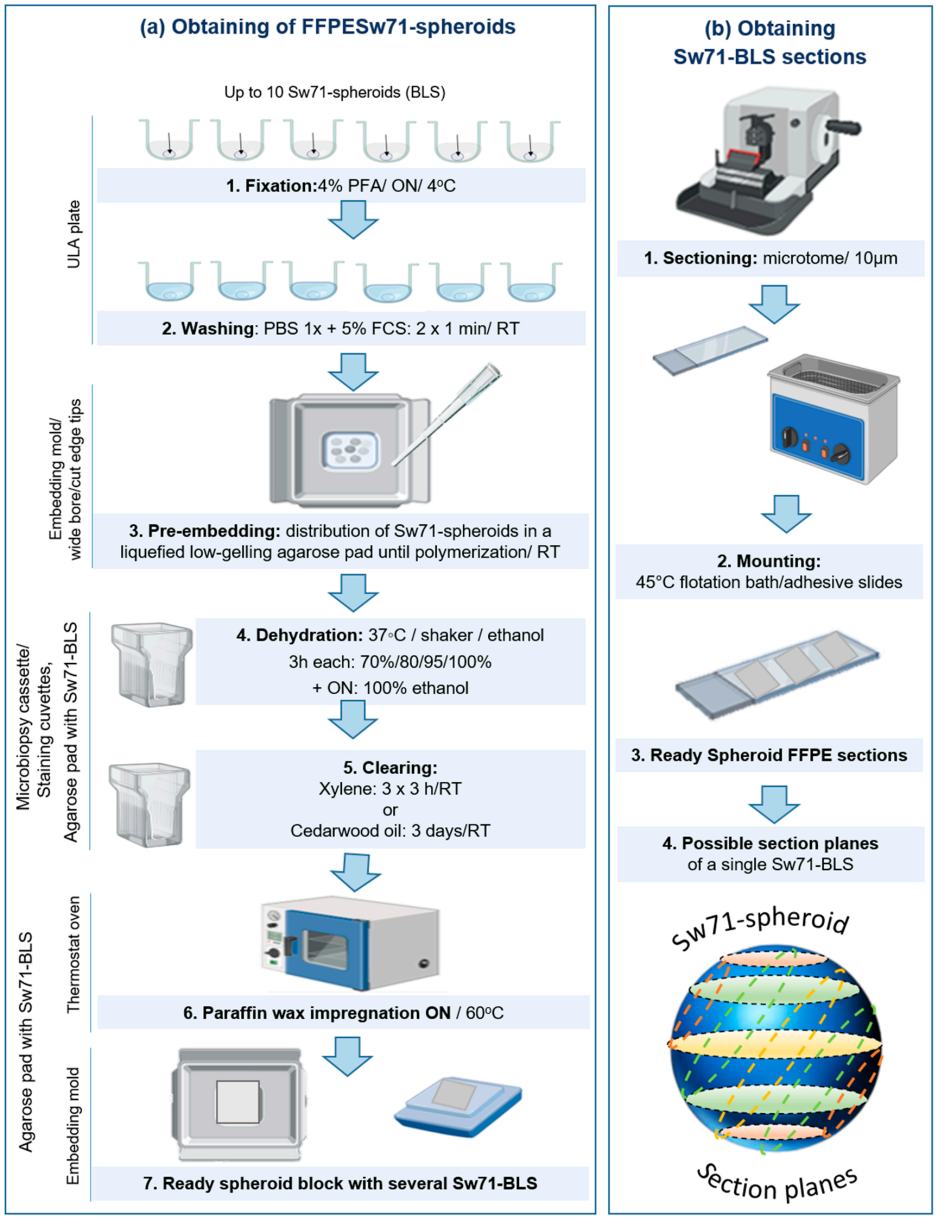



**Figure 1. Protocol for FFPE Sw71-BLS.** (**a**) **Procedure for embedding of Sw71-BLS** in paraffin wax including: PFA fixation (a.1), pre-embedding of up to 10 washed spheroids in a liquefied low-gelling agarose until polymerization of the matrix pad (a.2–3), dehydration through a graded scale of alcohols with increasing concentrations (a.4), clearing in xylene or cedarwood oil (a.5), infiltration in paraffin (a.6) and embedding in paraffin wax for a ready spheroid paraffin block, containing several Sw71-BLS (a.7). (**b**) **Procedure for sectioning of FFPE Sw71-spheroids:** obtaining of 10 µm sections (b.1) flattening and mounting on adhesive slides (b.2). Note that the ready Sw71-BLS serial sections contained multiple spheroids in the agarose matrix that are not aligned in a same plane (b.3–4). Theoretical planes for the sections of a sphere are given (b.4) to show that we do not expect only identical planes for each spheroid captured in a single spheroid block section.

### *2.3. Hematoxylin and Eosin Staining (H/E)*

FFPE sections of Sw71-BLS were deparaffinized in xylene (2 × 10 min) and rehydrated by immersion in alcohol baths of decreasing degree (100%, 95%, 80%, 70%), followed by wash in PBS and distilled water ($dH_2O$), 5 min in each. The sections were stained with hematoxylin and eosin (H/E) following standard protocol: cell nuclei staining with Ehrlich's hematoxylin (1 min) and differentiation in tap water (10 min), cytoplasm staining with 4% aqueous eosin solution (4 min), quick dehydration by rinsing in 70%, 80% and 95% and 1 min in 100% ethanol, clearing xylene (2 × 10 min) and mounting medium (Biomount DPX, Biognost, Zagreb, Croatia) and coverslip. The final preparations were observed under a microscope (Olympus Microscope BX51, Olympus Corporation, Hamburg, Germany) and photographed.

### *2.4. Immunohistochemistry (IHC)*

Selected sections of Sw71-spheroids (n = 3) were subjected to IHC for in situ detection of the epithelial cell adhesion molecule (EpCAM), human leucocyte antigen C (HLA-C) and G (HLA-G) within the spheroid structure. Each staining was repeated twice. A three-step biotin–streptavidin–enzyme method and UltraTek biotin-polyvalent streptavidin-horseradish peroxidase (HRP) visualization system (Ref.: AFN600-IFU, ScyTek, Logan, UT, USA) was used. In brief, the dewaxed and rehydrated sections were incubated with 10× diluted in PBS Super Block for inhibition of the non-specific binding. After washing (2 × 5 min/PBS/RT) the Sw71-spheroid sections were incubated with primary purified antibodies in appropriate dilution, overnight (ON), at 4 °C in humidified chamber as follows: anti-EpCAM (dilution 1:50, clone LEA15, Ref.: E-AB-71007, Elabscience, Houston, USA), anti-HLA-C (dilution 1:30, clone C-8, Ref.: sc-166088, SANTA CRUZ Biotechnology, Dalas, USA), and the anti-HLA-G (polyclonal rabbit, dilution 1:200, Ref.: E-AB-18031, Elabscience, Houston, USA). The endogenous biotin was blocked with Biotin Blocking Kit 10× diluted in PBS (ScyTek, Logan, UT, USA, Ref.: BBK-IFU). After washing the sections were incubated with biotinylated antibody (10 min/RT), washed and incubated with a streptavidin-HRP (10 min/RT). The chromogen 3,3′-diaminobenzidine tetrahydrochloride (DAB, 80× diluted, CRF Anti-Polyvalent HRP Polymer stain kit ScyTek, Logan, UT, USA, Ref. CPH080-IFU) was added to the washed slides (5 min/RT). Nuclei were counterstained with Ehrlich's hematoxylin (30 s) and the sections were dehydrated in increasing ethanol concentrations (70%, 80%, 95% and 100%, 5 min in each), cleared in xylene (2 × 5 min), and covered. For the negative control staining, the primary antibody was omitted. The final preparations were observed under a microscope (Olympus Microscope BX51, Olympus Corporation, Hamburg, Germany) and photographed. In addition to direct examination of bright field, the positive signal was analyzed and quantified using ImageJ, v.Fiji 7.1.4 [15,16]. We set up a threshold using the negative control digital signal and represent the positive trophoblasts as positive area from the selected view (signal-threshold, %) [16].

### *2.5. Statistical Analyses*

Statistics was processed with GraphPad Prism v.5.0 software using the Mann Whitney test. Data represent the average of at least three biological replicates and are presented as mean ± SD. Statistical significance is defined as $p < 0.05$ (*); $p < 0.005$ (**); $p < 0.001$ (***).

## 3. Results

### *3.1. Differentiation and Morphology of Sw71-Spheroids*

Following the standardized protocol, we observed the characteristic self-organization of the Sw71 EVT-like cells in multilayered, stable, round-shaped spheroids within 48 h (Figure 2). During the first 12 h there was Sw71 cell aggregation into a loose sphere

(Figure 2a,b) which become more condense until the 24th hour (Figure 2c) and undergoes additional compactization with cavitation until the 48th hour (Figure 2d). On day 0 the mean spheroid diameter was 1.190 ± 0.126 mm, and the surface was 1.226 ± 0.280 $mm^2$. On day 2 they were 0.345 ± 0.022 mm, and the surface was 0.141 ± 0.046 $mm^2$ demonstrating the characteristic significant compactization during differentiation respectively (Figure 2e,f).

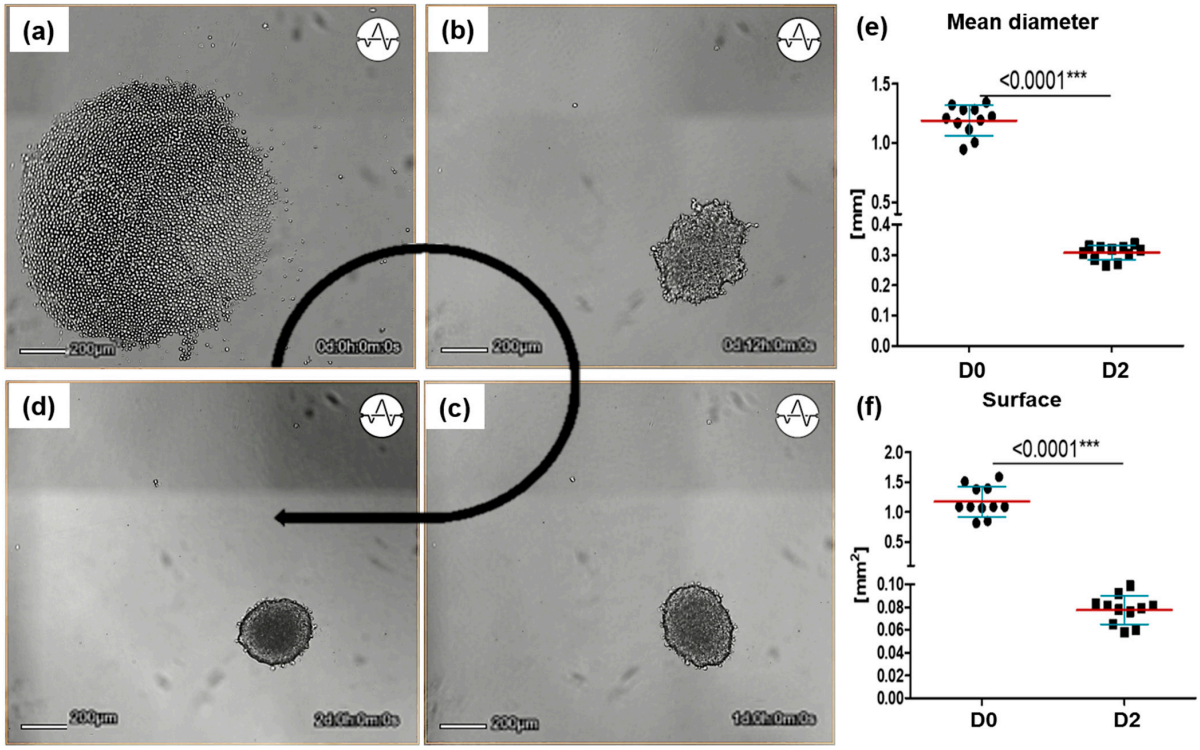



**Figure 2. Differentiation of Sw71-spheroids**: (**a**–**d**). Differentiation of Sw71-BLS monitored for 48 h with time-lapse live cells imaging system Omni (Axion Biosystems, Inc.,). During the first 12 h Sw71 cells aggregated loosely (**a**,**b**) till significant condensation at 24th hour (**c**) and additional compactization with cavitation (darkest central part) until the 48th hour (**d**). (**e**) Mean diameter of representative differentiated Sw71 BLS (n = 11). It is calculated as the average of the two largest diameters since the model is not a perfect sphere. (**f**) Surface of the same representative Sw71-spheroids (n = 11), calculated by the ECHO software (ECHO Pro, RVL100-M, Echo, San Diego, CA, USA). **Scale bar**: 200 µm. $p < 0.001$ (***).

### *3.2. Protocol for FFPE of Sw71-BLS*

The structures were proceeded for paraffin embedding according to protocol with several steps, shown in the workflow chart in Figure 1. It is important to note, that we used viable Sw71-spheroids, immediately after their differentiation (lasting 48 h). Stable for transfer intact Sw71-spheroids were fixed (ON/4 °C) in the ULA plate with 4% paraformaldehyde (PFA) in PBS pH 7.4. Of note some spheroids were fixed for 30 min/RT. The next day they were brought to RT, washed in PBS with 5% FCS and up to 10 Sw71-BLS were transferred, using a cut edge tip in 2% liquefied low-gelling temperature agarose (#A9045, Sigma-Aldrich) in embedding mold to form a block with several spheroids (up to ten). The agarose was left to solidify at room temperature. It was further processed as tissue preparation in a microbiopsy cassette at RT. In brief, the spheroid block was dehydrated through ethanol with increasing concentrations (70%, 80%, 95%, 100%), 3 h in each, with shaking. As last step of dehydration the agarose Sw71-spheroid block was left ON in new absolute ethanol. Then it was subjected to clearing with either xylene (Ref.: 1840, Valerus, Sofia, Bulgaria) for 3 × 3 h or Cedarwood oil (Ref.: 6965, Merck, Darmstadt, Germany) for 3 days. The Cedarwood oil is an alternative to make the Sw71-spheroid block translucent

for the spheroid cells to be well visible under light microscopy [17]. The Sw71-spheroid block was ON-infiltrated in liquid paraffin at 60 °C in thermostat oven (Memmert 100-800, Schvabach, Germany) and then embedded in paraffin wax. Few spheroids were proceeded without pre-embedding in 2% low-gelling agarose or 2% agar pad. The ready spheroid block, containing several Sw71-BLS was cut into 10 µm sections (Figure 1b(1–4)). Serial sections flatten in a flotation bath at 45 °C and mounted on Superfrost PLUS slides (Ref.: J1800AMNZ, Thermo Scientific, Waltham, MA USA). The intersection of a plane with a sphere is a circle. Therefore, the ready for staining serial Sw71-BLS sections contained multiple circle slices of spheroids in agarose matrix that are not aligned in a same plane (Figure 1b(4)).

### *3.3. Histological Examination of Sw71-BLS*

Our protocol for paraffin-embedding of micro-sized Sw71 BLS provided preserved cell morphology (Figure 3). The polymerized low-gelling temperature agarose from the spheroids' block is effectively infiltrated with paraffin but still distinguishable around each spheroid/group of spheroids in the sections. However, it does not interfere with the H/E staining (Figure 3a,b). The inclusion in the matrix of the agarose pad permits simultaneous embedding of several Sw71-spheroids in the block, each oriented in different plane (Figures 1b(4) and 3a). We did not observe cavity in any of the sections. Of note the entire structure and in particular the intact peripheral zone (arrows, Figure 3a,b), is better preserved as compared to directly embedded in paraffin Sw71-BLS (Figure 3c). High-magnification images show excellent cell morphology and intact periphery of the pre-embedded spheroids (Figure 3a,b, down). Notably, the 3 days clearing in cedarwood oil provides the easiest cutting and flattening of the sections. We did not get good paraffin infiltration with the agar pad, stored in 70% ethanol for up to two weeks and thus we were not able to obtain spheroid sections. The Sw71-spheroids were better preserved with the ON fixation on 4 °C as compared to 30 min/RT.

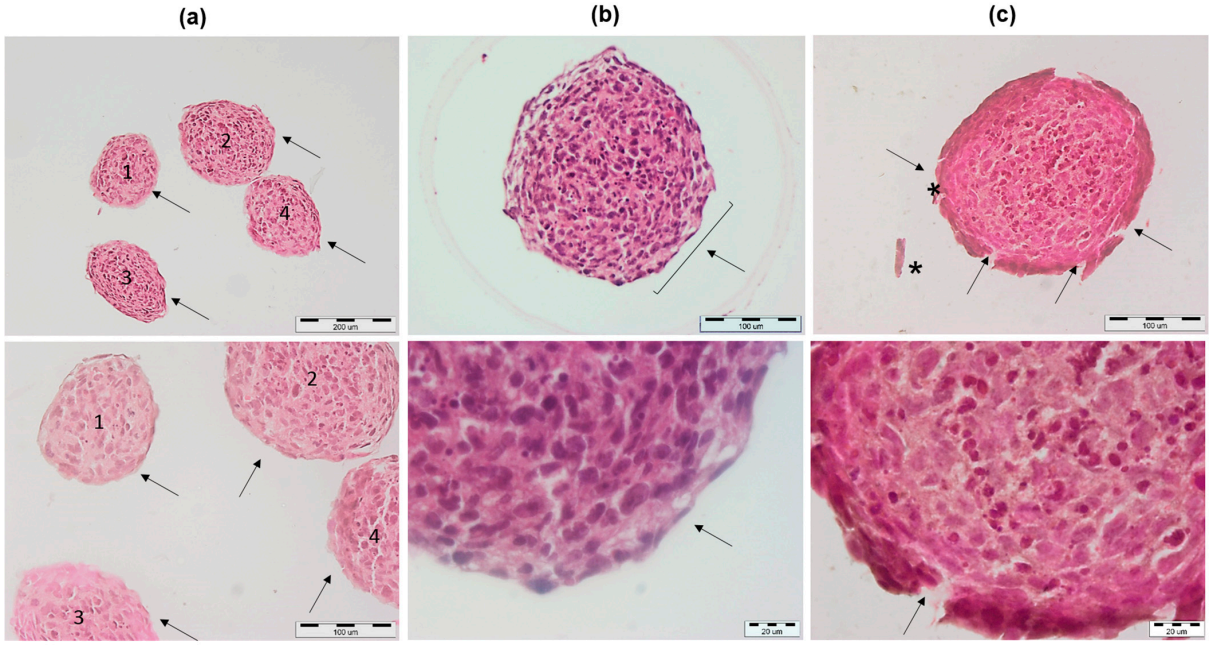



**Figure 3. Sw71-spheroid sections stained by H/E—representative for three preparations for each condition:** (**a**) A group of sections from 4 different spheroids without overlaps (arrows). Note that

each spheroid is from different part of the spheroid and in different planes. (**b**) Section from an agarose pre-embedded, paraffin-embedded Sw71-BLS at different magnifications. The spheroid is with preserved morphology and with intact peripheral zone (arrowed zone); (**c**) Section from directly embedded (without agarose matrix) in paraffin Sw71-BLS at different magnifications. Note the relatively preserved spheroid morphology but with breaks (arrows) in the peripheral zone and even with detached fragment (asterix). **Magnification:** (**a**) Up: 20×, down: 40×, (**b**,**c**) Up: 40×. down: 100×, Olympus Microscope BX51.

### *3.4. Expression of EpCAM, HLA-C, and HLA-G Molecules by Sw71 EVT-like Cells Within the Sw71-BLS*

The Sw71 trophoblasts within the spheroid structure were EpCAM, HLA-C, and HLA-G positive (Figure 4). Interestingly the most intensive signal for all the markers was observed preferentially in the peripheral trophoblasts (Figure 4b–d, arrows). Of note cells from couple peripheral layers were strongly EpCAM positive but only the outher layer was strongly HLA-C- and HLA-G-positive. These are the first trophoblasts to detach and migrate from the spheroid as differentiated EVT. The quantification of the digital signal, against the negative control threshold showed that only the Sw71 area from the selected view (positive signal minus threshold (red), 68%) expressed EpCAM (Figure 4a,b), HLA-C (54%, Figure 4a,c) and HLA-G (55%, Figure 4a,d) positive (Figure 4a,d).

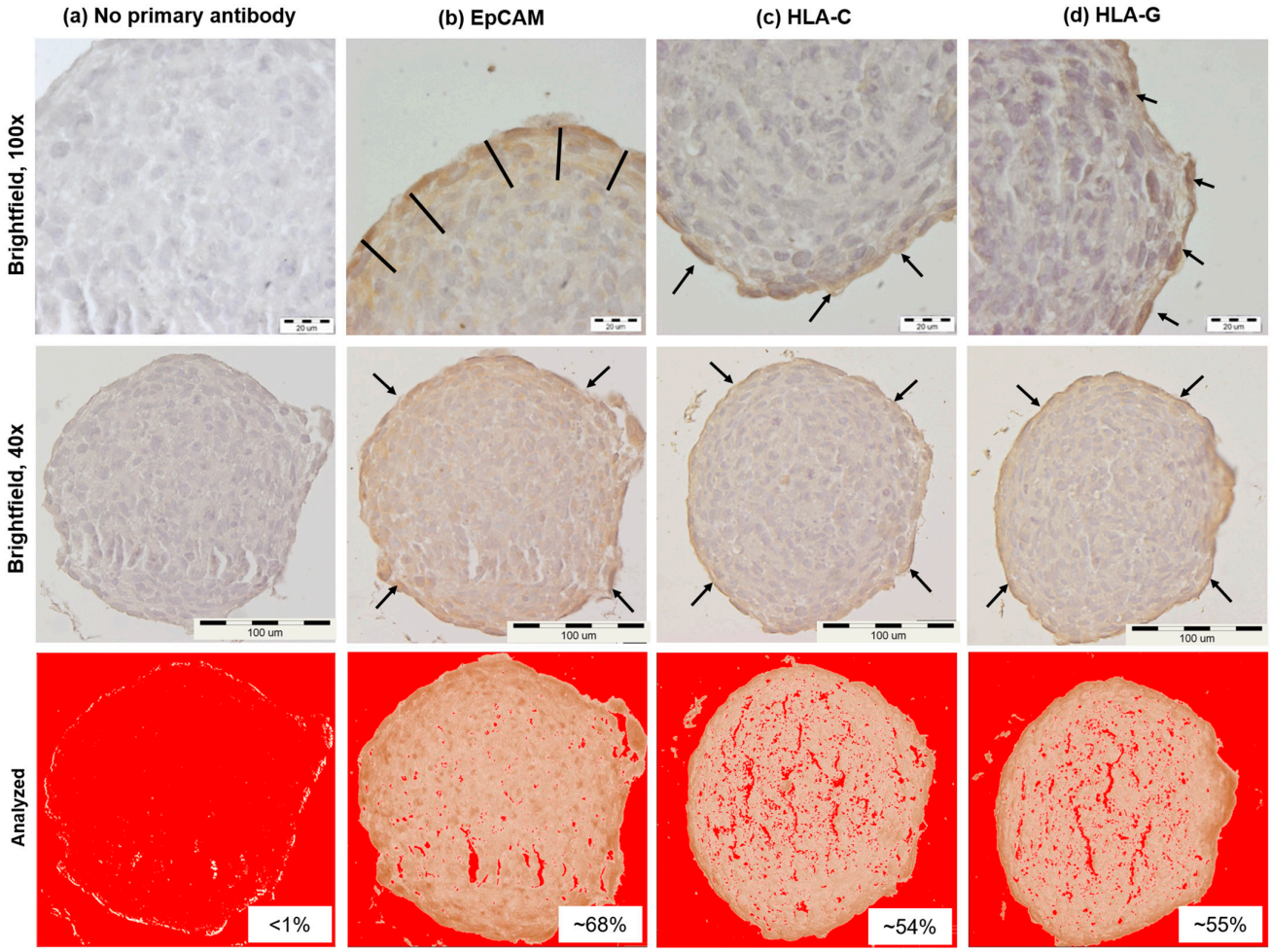



**Figure 4. Expression of EpCAM, HLA-C, and HLA-G by Sw71-BLS, shown by IHC—representative spheroids of three per each staining, repeated twice**. (**a**) Negative conrol: Sw71-spheroid section

without primary antibody with no significant background signal from the biotin-polyvalent-HRP visualization system. (**b**) EpCAM stained Sw71-spheroid section showing 68% positive trophoblast area from the selected view (signal-threshold (red), %, down). EpCAM signal was evenly distributed throughout the Sw71 spheroid with the most intensity in the peripheral layers of Sw71 cells (delineated by the lines, middle). (**c**) Expression of the HLA-C molecule by the 54% positive area of the Sw71-BLS (down). The outer layer was with the most intensive signal. (**d**) Expression of the HLA-G molecule by the 55% positive area with Sw71 cells (down). The most intensive signal for all the markers in the periphery of the Sw71-spheroid. Scale bar: Up: 20 µm, middle: 100 µm. The shown spheroids are representative of triplet per each staining, repeated twice.

## 4. Discussion

Spheroid cultures enable the co-existence of proliferative, quiescent and apoptotic states of the composing cells due to the architecture of the 3D construct and the varying access to oxygen and nutrients better resembling the in vivo conditions [5–7,18]. We have obtained stable, round shaped Sw71-spheroids that conform to the standardized parameters, with blastocyst-like morphology. The Sw71 blastocyst-like structures are a useful and biologically relevant in vitro 3D model for assessing the features and functionality (attachment, migration and invasion) of the trophoblast during human implantation [6,9–11,13]. By using this model important factors for human implantation were investigated. For example, it was confirmed that the human chorionic gonadotropin enhances the trophoblast–epithelial interaction [19] while the reticular stress and unfolded protein response prevention was shown to decrease the trophoblast cell invasion [20]. Trophoblast-educated B cells were shown to not express soluble factors that affect the invasion and migration activity of the Sw71 BLS. The Sw71 cells actually promote induction of a regulatory phenotype in B cells that can protect against detrimental T cell-mediated inflammation [21]. The Sw71-spheroids had served also to prove that the TNF-$\alpha$ regulated endometrial stroma secretome promotes trophoblast invasion [22]. A basic disadvantage of these 3D cultures is the restricted vitality. The Sw71 spheroids remain viable with preserved morphology up to 2 weeks [9].

Here we present a protocol for paraffin embedding for permanent histological preparation of the Sw71-BLS. The main challenges were the small size of the object and the preservation of the intact structures. The agarose pad in which the Sw71-BLS are pre-embedded, helps the operator to easily move all the spheroids at once during the processing for paraffin embedding. The inclusion of the small spherical structures directly in the liquefied low-gelling agarose and the processing per se might cause a bit shrinking. This was confirmed by some slightly deformed (not circle) sections. Another confirmation is that, although we had standard differentiation of the Sw71-spheroids and entirely sectioned in series spheroid blocks, we did not get sections with mean diameter $0.345 \pm 0.022$ mm or with well defined, typical for the model blastocyst-like cavity, shown previously by confocal microscopy [6]. Wong et al. have used similar preparation for embedding of HTR8/SVneo EVT -spheroids which led to similar results [18]. There are some differences from our protocol. For example, the spheroids' fixation is with 10% formalin within the ULA plates for 15 min/RT. We tested fixation for 30 min/RT and determined empirically that the overnight fixation at 4 °C with 4% PFA led to better preserved/stabilized Sw71-BLS. They directly mix the fixator in the well with 2% liquefied agar, mix and solidify on ice, fix additionally into 10% formalin for 48 h, and store in 70% ethanol until paraffin infiltration. In our experiments, washed spheroids, embedded in 2% agar, stored in 70% ethanol for up to two weeks, were no effectively infiltrated with paraffin wax and we were not able to obtain spheroid sections. Therefore, we switched to pre-embedding of washed spheroids in liquefied low-gelling agarose and more gentle dehydration and clearing steps. In contrast to others using agarose pad embedding [23], we do not use specifically prepared, time consuming or more expensive negative mold to obtain a microarray of equally distributed

spheroids for high-throughput analysis of many 3D structures at a time. We embeded up to 10 spheroids in a block. The best morphology and the optimal quality of the obtained histological sections was reached with pre-embedding in an agarose pad, followed by paraffin infiltration and clearing in xylene or cedarwood oil. The agarose matrix sustained the integrity of the several Sw71-spheroids. As the Sw71-BLS are placed consecutively but fast, in the serial cuts of the spheroid block we get enough sections from different parts of the Sw71-spheroid, oriented in varying planes. Of note others reach less spheroids in different planes on a single microarray section [23]. The ability to obtain serial sections from the spheroid block indicates that the paraffin embedding was carried out as correctly as possible, and the low-gelling agarose had good permeability to xylene/cedarwood oil and subsequently to paraffin wax. Other authors describe direct paraffin embedding of fixed blastocysts [24]. In our experiments, direct paraffin embedding of fixed and washed Sw71-spheroids resulted in sections with spheroids with impaired peripheral zone. Therefore, we recommend matrix pre-embedding of the Sw71-BLS before paraffin infiltration. The embedding in low-gelling agarose of invading spheroids might be useful as well. This will allow obtaining of some spheroid sections in planes, containing both the sliced spheroid and outgrowing migrating/invading EVT in permanent histological preparations for in depth IHC studies.

We tested standard protocols for H/E and IHC staining of Sw71-spheroid sections and demonstrate the feasibility of available protocols for quantification of IHC images with popular software for image analyses. We believe these might serve as fundament for further and in-depth studies of EVT structure and functions. In particular, we showed that EVT from Sw71-spheroid were EpCAM, HLA-C and HLA-G positive. EpCAM positivity testifies their epithelial origin but is also involved in cell signaling, proliferation, differentiation and migration [25]. In early first trimester the cytotrophoblasts within the columns maintaining pools of dividing progenitor cells are positive for EpCAM [26]. As EVT-like cells Sw71 trophoblast express a tolerogenic HLA pattern including negativity for the classical polymorphic HLA class I molecules except for HLA-C and positivity for the non-classical invariant HLA-G [13,14]. Indeed, most of the cells in the paraffin embedded Sw71-spheroids were also HLA-C and HLA-G positive. The concomitant EpCAM expression confirms the possibility of Sw71 EVT-like cells for constant epithelial-mesenchymal and reverse transitions for effective invasion of the decidua during the implantation [13,14]. This is crucial for the successful placentation in vivo. The highest signal for all three markers we gained in the periphery of the Sw71-spheroid sections. It should be noted that here we do not have an entire sphere but only thin slices from it in a single plane. Namely in the peripheral Sw71-spheroid layers are the EVT that will first detach from the Sw71-BLS surface to migrate and invade between decidual stromal cells. They model the invading EVT trophoblast in the very first steps of human implantation [6,9–11,13].

Overall, the embedding of the Sw71-spheroids does not interfere with their quality as a trophoblast model for an implanting human blastocyst. The embedding of invading Sw71-spheroids is an intriguing perspective for spatial IHC analyses for the expression of important markers for trophoblast function during the very early human implantation, inaccessible for in vivo analyses [6].

## 5. Conclusions

We have demonstrated that it is possible to obtain high-quality histological sections of Sw71-BLS in feasible, low-scale, inexpensive, and reproducible manner, which ensures their use in subsequent histological and IHC analyses. Our protocol does not allow the processing of numerous samples for high-throughput histological analysis/studies, due to manual processing. However, it might be further optimized to embed migrating/invading

structures. The aim is to obtain snapshot of implantation steps in permanent histological preparations that could be used for in depth IHC studies. Fortunately, there is increasing evidence of the integration of sophisticated immunohistochemistry techniques with high-throughput 3D spheroid culture technologies, which will allow researchers to efficiently study the expression of multiple biomarkers with spatial localization in 3D structures.

**Author Contributions:** Conceptualization, M.A. and T.D.; methodology, M.A., M.I., M.M., A.T. and T.D.; software, M.A., A.T. and T.D.; validation, M.A., M.M. and M.I.; investigation, M.A., T.D., M.M. and A.T.; data curation, M.A.; writing—original draft preparation, M.A., M.I. and M.M.; writing—review and editing, T.D.; visualization, M.A., M.I., M.M. and A.T.; supervision, T.D.; project administration, T.D.; funding acquisition, T.D. All authors have read and agreed to the published version of the manuscript.

**Funding:** This research was funded by the Bulgarian National Science Fund within the National Science Program VIHREN, contract number KP-06-DV-3.

**Institutional Review Board Statement:** Not applicable.

**Informed Consent Statement:** Not applicable.

**Data Availability Statement:** The original contributions presented in this study are included in the article. Further inquiries can be directed to the corresponding author.

**Acknowledgments:** The normal, immortalized, 1st-trimester human placenta Sw71 (#CVCL_D855) trophoblast cell line used in the study was kindly provided by Gil Mor.

**Conflicts of Interest:** The authors declare no conflicts of interest.

## Abbreviations

The following abbreviations are used in this manuscript:

| | |
|---|---|
| BLS | Blastocyst-like surrogate |
| EVT | Extravillous trophoblast |
| FFPE | Formalin-fixed paraffin-embedded |
| H/E | Hematoxylin & eosin |
| IHC | Immunohistochemistry |
| 3D | Three dimensional |
| ULA | Ultra-low attachment |
| PFA | Paraformaldehyde |
| RT | Room temperature |
| EpCAM | Epithelial cell adhesion molecule |
| HLA | Human leucocyte antigen |
| HRP | Horseradish peroxidase |

## References

1. Chard, T. Frequency of implantation and early pregnancy loss in natural cycles. *Baillière's Clin. Obstet. Gynaecol.* **1991**, *5*, 179–189. [CrossRef] [PubMed]
2. Macklon, N.S.; Geraedts, J.P.M.; Fauser, B.C.J.M. Conception to ongoing pregnancy: The "black box" of early pregnancy loss. *Hum. Reprod. Update* **2002**, *8*, 333–343. [CrossRef] [PubMed]
3. Wang, X.; Chen, C.; Wang, L.; Chen, D.; Guang, W.; French, J. Conception, early pregnancy loss, and time to clinical pregnancy: A population-based prospective study. *Fertil. Steril.* **2003**, *79*, 577–584. [CrossRef] [PubMed]
4. Muter, J.; Lynch, V.J.; McCoy, R.C.; Brosens, J.J. Human embryo implantation. *Development* **2023**, *150*, dev201507. [CrossRef]
5. Schmidt, A.; Morales-Prieto, D.M.; Pastuschek, J.; Fröhlich, K.; Markert, U.R. Only humans have human placentas: Molecular differences between mice and humans. *J. Reprod. Immunol.* **2015**, *108*, 65–71. [CrossRef]
6. Dimova, T.; Alexandrova, M.; Vangelov, I.; You, Y.; Mor, G. The modeling of human implantation and early placentation: Achievements and perspectives. *Hum. Reprod. Update* **2024**, *31*, 133–163. [CrossRef]

7. Fang, Y.; Eglen, R.M. Three-Dimensional Cell Cultures in Drug Discovery and Development. *SLAS Discov.* **2017**, *22*, 456–472. [CrossRef]
8. Matthews, K.R.; Moralí, D. National human embryo and embryoid research policies: A survey of 22 top research-intensive countries. *Regen. Med.* **2020**, *15*, 1905–1917. [CrossRef]
9. Alexandrova, M.; Manchorova, D.; You, Y.; Mor, G.; Dimitrova, V.; Dimova, T. Functional HLA-C expressing trophoblast spheroids as a model to study placental–maternal immune interactions during human implantation. *Sci. Rep.* **2022**, *12*, 10224. [CrossRef]
10. Holmberg, J.C.; Haddad, S.; Wünsche, V.; Yang, Y.; Aldo, P.B.; Gnainsky, Y.; Granot, I.; Dekel, N.; Mor, G. An In Vitro Model for the Study of Human Implantation. *Am. J. Reprod. Immunol.* **2012**, *67*, 169–178. [CrossRef]
11. You, Y.; Stelzl, P.; Zhang, Y.; Porter, J.; Liu, H.; Liao, A.H.; Aldo, P.B.; Mor, G. Novel 3D in vitro models to evaluate trophoblast migration and invasion. *Am. J. Reprod. Immunol.* **2019**, *81*, e13076. [CrossRef]
12. Straszewski-Chavez, S.L.; Abrahams, V.M.; Alvero, A.B.; Aldo, P.B.; Ma, Y.; Guller, S.; Romero, R.; Mor, G. The Isolation and Characterization of a Novel Telomerase Immortalized First Trimester Trophoblast Cell Line, Swan 71. *Placenta* **2009**, *30*, 939–948. [CrossRef] [PubMed]
13. Alexandrova, M.; Manchorova, D.; You, Y.; Terzieva, A.; Dimitrova, V.; Mor, G.; Dimova, T. Validation of the Sw71-spheroid model with primary trophoblast cells. *Am. J. Reprod. Immunol.* **2023**, *90*, e13800. [CrossRef] [PubMed]
14. Alexandrova, M.; Manchorova, D.; Dimova, T. Immunity at maternal-fetal interface: KIR/HLA (Allo)recognition. *Immunol. Rev.* **2022**, *308*, 55–76. [CrossRef] [PubMed]
15. Schindelin, J.; Arganda-Carreras, I.; Frise, E.; Kaynig, V.; Longair, M.; Pietzsch, T.; Preibisch, S.; Rueden, C.; Saalfeld, S.; Schmid, B.; et al. Fiji: An open-source platform for biological-image analysis. *Nat. Methods* **2012**, *9*, 676–682. [CrossRef]
16. Shang, C. Analyze Immunohistochemistry Images in ImageJ 2018. Available online: https://resources.finalsite.net/images/v1567623985/lsuhscshreveportedu/awsil3hxeld0mkym4bzl/immunohistochemistrystaining.pdf (accessed on 9 April 2025).
17. Thamilselvan, S.; Sherlin, H.J.; Jayaraj, G.; Don, K.R.; Santhanam, A. Cedarwood oil as an alternative to xylene as a clearing agent in histopathological tissue processing—A comparative study. *J. Oral Maxillofac. Pathol.* **2021**, *25*, 299–305. [CrossRef]
18. Wong, M.K.; Wahed, M.; Shawky, S.A.; Dvorkin-Gheva, A.; Raha, S. Transcriptomic and functional analyses of 3D placental extravillous trophoblast spheroids. *Sci. Rep.* **2019**, *9*, 12607. [CrossRef]
19. Racicot, K.E.; Wünsche, V.; Auerbach, B.; Aldo, P.; Silasi, M.; Mor, G. Human chorionic gonadotropin enhances trophoblast-epithelial interaction in an in vitro model of human implantation. *Reprod. Sci.* **2014**, *21*, 1274–1280. [CrossRef]
20. Grasso, E.; Gori, S.; Soczewski, E.; Fernández, L.; Gallino, L.; Vota, D.; Martínez, G.; Irigoyen, M.; Ruhlmann, C.; Lobo, T.F.; et al. Impact of the Reticular Stress and Unfolded Protein Response on the inflammatory response in endometrial stromal cells. *Sci. Rep.* **2018**, *8*, 12274. [CrossRef]
21. Guzman-Genuino, R.M.; Dimova, T.; You, Y.; Aldo, P.; Hayball, J.D.; Mor, G.; Diener, K.R. Trophoblasts promote induction of a regulatory phenotype in B cells that can protect against detrimental T cell-mediated inflammation. *Am. J. Reprod. Immunol.* **2019**, *82*, e13187. [CrossRef]
22. You, Y.; Stelzl, P.; Joseph, D.N.; Aldo, P.B.; Maxwell, A.J.; Dekel, N.; Liao, A.; Whirledge, S.; Mor, G. TNF-α Regulated Endometrial Stroma Secretome Promotes Trophoblast Invasion. *Front. Immunol.* **2021**, *12*, 737401. [CrossRef]
23. Gabriel, J.; Brennan, D.; Elisseeff, J.H.; Beachley, V. Microarray Embedding/Sectioning for Parallel Analysis of 3D Cell Spheroids. *Sci. Rep.* **2019**, *9*, 16287. [CrossRef]
24. Usón, A.; López-Morató, M.; Mijares, J.; Sánchez-Mateos, S.; Sánchez-Margallo, F.M.; Álvarez, I.S.; Hernández, N. Histological cut of a paraffin-embedded blastocyst: Optimized protocol for murine blastocysts. *MethodsX* **2020**, *7*, 100767. [CrossRef]
25. Ng, V.Y.; Ang, S.N.; Chan, J.X.; Choo, A.B.H. Characterization of epithelial cell adhesion molecule as a surface marker on undifferentiated human embryonic stem cells. *Stem Cells* **2010**, *28*, 29–35. [CrossRef]
26. Wong, F.T.M.; Lin, C.; Cox, B.J. Cellular systems biology identifies dynamic trophoblast populations in early human placentas. *Placenta* **2019**, *76*, 10–18. [CrossRef]


**Disclaimer/Publisher's Note:** The statements, opinions and data contained in all publications are solely those of the individual author(s) and contributor(s) and not of MDPI and/or the editor(s). MDPI and/or the editor(s) disclaim responsibility for any injury to people or property resulting from any ideas, methods, instructions or products referred to in the content.